
Li isotopic variations in single pyroxenes from the Northwest Africa 480 shergottite (NWA 480): a record of degassing of Martian magmas?

P. Beck^{1*}, J. A. Barrat², M. Chaussidon³, Ph. Gillet¹ and M. Bohn⁴

¹Laboratoire des Sciences de la Terre, CNRS UMR 5570, Ecole Normale Supérieure de Lyon, 46 allée d'Italie, 69364, Lyon Cedex 7, France

²CNRS UMR 6112 (Géodynamique et Planétologie) and C NRS UMR 6538 (Domaines Océaniques), U.B.O.-I.U.E.M., place Nicolas Copernic, F-29280, Plouzané Cedex, France

³CRPG-CNRS UPR 2300, 15 rue Notre-Dame des Pauvres, 54501, Vandœuvre-les-Nancy Cedex, France

⁴Ifremer-Centre de Brest, (CNRS-UMR 6538), BP70, 29280, Plouzané Cedex, France

*: Corresponding author : pbeck@ens-lyon.fr

Abstract: Lithium abundances and isotopic compositions were measured by ion microprobe in individual grains of pyroxene, and in a few maskelynites and Ca-phosphates grains, from the Martian meteorite Northwest Africa 480 (NWA 480).

In pyroxenes Li abundances are nearly constant from core to rim with concentrations ranging between 3 and 4 µg/g. In contrast, a significant isotopic zoning is observed with $\delta^7\text{Li}$ values increasing within single crystals from not, vert, similar -17% in the core to not, vert, similar $+10\%$ in the rim, most of the variability being observed in the core. Plagioclase (now maskelynite) and phosphate crystals, which co-crystallized with the pyroxene rims, display similar $\delta^7\text{Li}$ values. Because of the incompatible behavior of Li, the present constancy of Li concentrations within zoned pyroxenes rules out any simple crystallization model in a closed system for Li. The large Li isotopic variations observed within pyroxenes support this conclusion. There is no evidence in support of secondary alteration of NWA 480 to explain the Li isotopic variations, which thus most likely reflect magmatic processes on Mars. Degassing might explain the Li systematics observed in NWA 480 pyroxenes. Because Li has a strong affinity with water-rich fluids, a significant loss of Li from NWA 480 parental melt can happen upon melt emplacement and cooling. Such a Li loss could compensate the effect of crystal fractionation and thus help to maintain constant the Li content of the melt. Li isotopic fractionation is anticipated to accompany this process, ^7Li being depleted relative to ^6Li in the volatile phase. The magnitude of the isotopic change of the fractionating melts is difficult to predict because it depends on the value of the Li isotopic fractionation and on the amount of Li loss, but at first glance it seems consistent with the increase of $\delta^7\text{Li}$ values observed in NWA 480 pyroxenes with increasing fractionation. The present data suggest that degassing prevailed not only during the crystallization of shergottites like Zagami and Shergotty, but also during the crystallization of the other types of basaltic shergottites.

Keywords: variations, Geochemistry / Lithium / Isotopic composition / Pyroxene / Magma / Mars planet

1. INTRODUCTION

Naturally delivered Martian samples are available in the form of a group of ~25 meteorites that were inferred on geochemical grounds to come from this planet (see Treiman et al. (2000) and McSween (2002) for updated reviews). Most of these meteorites, the so-called shergottites, are basaltic lavas or cumulates indicating a recent magmatic activity on Mars because of their young ages (~170 Ma for most of the shergottites, e.g. Borg et al., 2002 and references therein). These meteorites are thus probes of the Martian mantle and are especially important objects to try to constrain the amount of volatiles, in particular magmatic water, transferred from the mantle to the surface.

Did Martian magmas significantly degas ? Bulk shergottites are dry, but the presence of water in their parental melts was inferred in order to explain the simultaneous crystallization of augite and pigeonite observed in some of them (McSween et al., 2001). Dann et al. (2001) have documented this feature experimentally and concluded that the parental magma of Shergotty contained about 1.8 wt% water. Therefore, if shergottitic magmas were hydrous, they have lost most, if not all, of their water through degassing.

Pyroxenes are good recorders of the crystallization history of their parental melts. For shergottites, the trace and minor element contents of the pyroxenes were successfully used to constrain the chemical composition of the parental liquids, the crystallization sequence of the various mineral phases and the oxygen fugacity during magmatic cooling (e.g. Wadhwa et al., 1994, 2001; Wadhwa, 2001). Furthermore, it was suggested by Lentz et al. (2001) that the decrease of Li and B contents, observed from cores to rims of pyroxenes in basaltic shergottites Shergotty and Zagami, was due to Li- and B-loss during water degassing. In fact the strong affinity of Li and B with water-rich fluids (e.g. Brenan et al., 1998b) make them potential tracers of degassing.

Because Shergotty and Zagami are petrographically similar, it is crucial to extend these observations to shergottites of different types. Therefore, we studied in detail Northwest Africa 480 (NWA 480), a basaltic shergottite recently discovered in Moroccan Sahara (Barrat et al., 2002). NWA 480 displays some specific features not observed in Shergotty or Zagami. The pyroxenes are large (millimeter-sized) and exhibit one of the widest ranges of compositions described so far in Martian meteorites. They are thus very suitable for an in-situ ion microprobe study. Lithium concentrations and isotopic compositions were systematically determined from core to rim of a crystal in order to obtain additional constraints which might help to better understand the factors controlling the geochemical behavior of Li in Martian magmas.

2. ANALYTICAL PROCEDURES

Back-Scattered Electron (BSE) images were obtained with a JEOL JSM6301-F scanning electron microscope at SCIAM (Angers). Major and minor element abundances were measured using a CAMECA SX50 electron microprobe (IFREMER-Centre de Brest). Analyses were obtained using mineral and oxide standards at an accelerating voltage of 15 kV, a probe current of 12 nA and a one micron beam diameter. Compositions were determined in the same regions where ion probe measurements were performed.

Li analyses were performed using the CAMECA IMS 3f ion microprobe at the CRPG-CNRS (Nancy). The technique used was previously developed for B and Li isotopic analyses (Chaussidon et al., 1997; Chaussidon and Robert, 1998; Decitre et al., 2002). A thick section of the sample was prepared in order to avoid any possibility of contamination from epoxy in cracks. This section was polished down to 1 micrometer using diamond paste and ultrasonically rinsed in alcohol and distilled water before gold coating. Positive ${}^6\text{Li}$ and ${}^7\text{Li}$ ions produced by the sputtering of a 10kV primary O^- beam ($\approx 60\text{nA}$ and $\approx 25\mu\text{m}$ diameter)

were accelerated at 4.5 kV and analyzed, with the energy slit centered and fully opened, at a low mass resolution ($M/\Delta M \approx 1000$) sufficient to remove any possible interference (e.g. ${}^6\text{LiH}^+$ or ${}^{28}\text{Si}^{4+}$) on the Li peaks. The Li concentrations were determined from measurements made in a different session than isotopic analyses and using different settings so that they do not correspond to exactly the same sputtered volume. However the primary beam had a very similar size ($\approx 20\text{nA}$ and $\approx 20\mu\text{m}$ diameter) as used for isotopic analyses and it was placed in the center of the existing spots (precision $\approx \pm 2 \mu\text{m}$). The Li concentrations were obtained from the measurement of the ${}^7\text{Li}^+/{}^{30}\text{Si}^+$ ratios with $M/\Delta M \approx 500$ and using an energy filtering of $-80 \pm 10 \text{ V}$.

The calibration of ion yields and instrumental mass fractionation for the determination of Li concentrations and isotopic compositions respectively, was performed on a set of three natural pyroxene minerals previously developed for this purpose (Decitre et al., 2002). These pyroxenes are an orthopyroxene (Opx BZ226, $3.7 \mu\text{g/g}$ Li and $\delta^7\text{Li} = -4.1 \pm 0.5\text{‰}$) and two clinopyroxenes (augite CpxBZ226, $5.9 \mu\text{g/g}$ Li and $\delta^7\text{Li} = -4.2 \pm 0.5\text{‰}$; augite CpxBZCG, $\delta^7\text{Li} = +10.5 \pm 0.5\text{‰}$).

The ion yield of Li relative to Si is defined as the ratio of positive ion intensities of Li to Si measured by ion probe relative to their real atomic concentration ratio in the mineral, i.e. $\text{yield Li} = (\text{Li}^+/\text{Si}^+) / (\text{Li}/\text{Si})$. This yield was determined, from four measurements of Opx BZ226 and Cpx BZ226 standards, at a value of 0.985 ± 0.047 and is very close to the value of 1.32 determined using slightly different analytical conditions (e. g. offset of $-77 \pm 19\text{V}$) on the NBS 610 glass (Hinton, 1990). Because the uncertainty based on counting statistics on the Li^+/Si^+ ratio is generally at the level of a couple of percent, the Li concentrations given in Table 2 can be considered reliable at $\pm 5\%$ (1 sigma). The Li concentrations determined by ion probe in the different mineral phases are consistent with bulk Li concentration of NWA 480 ($2.93 \mu\text{g/g}$, Barrat et al., 2002).

The instrumental mass fractionation of Li isotopes is defined as the ratio between the isotopic ratio of Li positive ions measured by ion probe relative to the true Li isotopic ratio in the minerals, i.e. $\alpha_{\text{inst}}^{\text{Li}} = ({}^7\text{Li}^+ / {}^6\text{Li}^+) / ({}^7\text{Li} / {}^6\text{Li})$. The value of $\alpha_{\text{inst}}^{\text{Li}}$ and the possible matrix effects on $\alpha_{\text{inst}}^{\text{Li}}$ were determined from the analysis of the three pyroxenes standards. This calibration (Fig. 1) shows that (i) $\alpha_{\text{inst}}^{\text{Li}}$ is stable within $\pm 1.5\%$ (1 sigma) for a given Cpx (see cpx BZ226 in figure 1), (ii) no significant (in excess of $\pm 1.5\%$) matrix effect on $\alpha_{\text{inst}}^{\text{Li}}$ is observed between opx and cpx or within cpx and (iii) $\alpha_{\text{inst}}^{\text{Li}}$ is constant within $\pm 1.5\%$ over a 15 % variation range of the ${}^7\text{Li}/{}^6\text{Li}$ ratio. Finally it is apparent that contrary to other elements, the instrumental mass fractionation of Li is positive: this peculiarity has been previously noted (e.g. Chaussidon et al., 1997) and does not affect the quality of Li isotopic measurements by ion microprobe. The Li isotopic ratios are given in Table 2 in delta units using the $\delta^7\text{Li}$ notation ($\delta^7\text{Li} = (({}^7\text{Li}/{}^6\text{Li}_{\text{sample}}) / ({}^7\text{Li}/{}^6\text{Li}_{\text{LSVEC}}) - 1) \times 1000$), LSVEC being the international carbonate standard for Li isotopes (${}^7\text{Li}/{}^6\text{Li}_{\text{LSVEC}} = 12.0192$, Flesh et al., 1973). The counting statistics on Li isotopic ratios for the different minerals of NWA 480 were generally better than $\pm 1.5\%$ (1 sigma). Thus, relative Li isotopic variations in NWA 480 of $\pm 3\%$ are significant at one sigma, while the total uncertainty of the $\delta^7\text{Li}$ values given in Table 2 relative to the LSVEC international standard includes (i) the errors due to counting statistics, (ii) the error on the determination of $\alpha_{\text{inst}}^{\text{Li}}$ (Fig 1) and (iii) the error on the $\delta^7\text{Li}$ of standards used to determine $\alpha_{\text{inst}}^{\text{Li}}$. Assuming that these three errors add in a quadratic way, a total uncertainty of $\pm 2.2\%$ (1 sigma) relative to LSVEC can be estimated for the present data. However note again that relative variations of the $\delta^7\text{Li}$ values can be detected at better than $\pm 1.5\%$ as demonstrated (i) by the duplicates made on a large pyroxene crystal (e.g. $\delta^7\text{Li} = -15.1\%$ for spot 13 in profile A-B and $\delta^7\text{Li} = -16.5$ for spot 28 in profile C-D, see Fig. 2 and Table 2) and (ii) by the constancy of the $\delta^7\text{Li}$ values measured in the cores of the different

pyroxene crystals studied (-17.3‰ for core of pyroxene 1, -17.7‰ for core of pyroxene 2 and -17.4‰ for core of pyroxene 3). Because the limitation on the precision of the Li isotopic measurements is obviously the counting statistics, a significant improvement of this precision seems unlikely in the near future unless multi-collection isotopic measurements are developed on a large radius type IMS 1270 ion microprobe.

Finally, $\delta^7\text{Li}$ values are also given in Table 2 for a few maskelynite and phosphate grains. These measurements were made in order to check that at first order no unexpected $\delta^7\text{Li}$ anomaly was present in these two minerals. These $\delta^7\text{Li}$ data must only be considered relative to this objective. In fact, theoretically these $\delta^7\text{Li}$ values cannot be assumed as precise as the pyroxene $\delta^7\text{Li}$ values, as no plagioclase or phosphate standards was available to check the matrix effect on $\alpha_{\text{inst}}^{\text{Li}}$. Thus the value of $\alpha_{\text{inst}}^{\text{Li}}$ used to correct the Li isotopic ratio on maskelynite and apatite was that determined on pyroxene standards. However the similarity between the $\delta^7\text{Li}$ of plagioclase and apatite co-crystallizing with pyroxene (see Fig. 7) argues against an important additional matrix effect in these two mineral phases.

3. RESULTS

NWA 480 is a fresh basaltic shergottite (Barrat et al., 2002). It is coarse-grained and consists mainly of large pyroxene crystals and maskelynite (amorphous plagioclase) (Fig. 2). Other accessory phases are phosphates, oxides (ilmenite and chromite) and silica. The compositional trend shown by pyroxenes is complex, with a Mg-rich core ($\text{En}_{77}\text{Fs}_{20}\text{Wo}_3$ - $\text{En}_{65}\text{Fs}_{29}\text{Wo}_6$) surrounded by a Mg-rich augite band (typically $\text{En}_{41}\text{Fs}_{29}\text{Wo}_{30}$), and finally zoned toward a pigeonite rim sometimes with a Mg-poor composition ($\text{En}_5\text{Fs}_{84}\text{Wo}_{11}$). All the plagioclase crystals were transformed into maskelynite during shock metamorphism and display limited zoning ($\text{An}_{42-50}\text{Ab}_{54-48}\text{Or}_{2-4}$).

3.1. Li concentrations

Li abundances were only measured in pyroxenes whose large sizes enabled numerous measurements to be made in the same crystal. The entire range of major element variation displayed by NWA 480 pyroxenes was sampled by ion probe measurements (Fig. 3). Two profiles were obtained on a large pyroxene crystal (Fig. 2). The profile A-B followed the long axis of the crystal, but did not cross the whole zoning. The second one (profile C-D) was made in order to analyze the augite band and the Fe-rich pigeonite rim. Except for a single point in the A-B profile (spot 12 having 5.5 $\mu\text{g/g}$ Li and being not situated on a specific crack or inclusion in the pyroxene), Li displays a restricted range of concentrations with values between 2 and 4 $\mu\text{g/g}$. These are in reasonable agreement with the bulk meteorite concentration (2.93 $\mu\text{g/g}$) as measured by Barrat et al. (2002). These Li concentrations are within the range measured for Shergotty and Zagami pyroxenes (1.68 $\mu\text{g/g}$ to 8.15 $\mu\text{g/g}$ Lentz et al., 2001) but the negative correlation between TiO_2 and Li observed in them is not present in NWA 480 pyroxenes (Fig. 4).

3.2. Li isotopic compositions

Two profiles were analyzed for Li isotopic compositions (Fig. 5 and Table 1). The $\delta^7\text{Li}$ values increase progressively from -17.3 ‰ in the core to $+9.8$ ‰ in the rim of the crystal. Core-rim analyses were also performed on two other pyroxene crystals which both display a similar trend in isotopic composition (Table 1). As shown in figures 5 and 6 the Li isotope variations recorded by the pyroxenes are decoupled from the Li concentrations, the $\text{fe}\#$ ($=100 \text{ Fe}/(\text{Fe}+\text{Mg})$, atomic), or any other major element concentration. The $\delta^7\text{Li}$ variations can be divided in two parts (Fig. 6): from $\text{fe}\# = 21$ to 30, the $\delta^7\text{Li}$ ratios increase regularly from -17 to about $+7$ ‰; for $\text{fe}\#$ ratios greater than 30, the $\delta^7\text{Li}$ ratios are less variable and range irregularly between $+2$ and $+10$ ‰. The limit between these two parts at $\text{fe}\#=30$ does not coincide with a major change of the pyroxene composition such as the appearance of augite ($\text{fe}\#$ about 35) or the beginning of the co-crystallization of Fe-pigeonite and plagioclase at a $\text{fe}\#$ -value close to 50, as indicated by the behavior of aluminum (Fig. 6).

Textural relationships and rare earth element microdistributions indicate that feldspar and phosphates have co-crystallized with the pyroxene rims (Croizat et al., 2001; Barrat et al., 2002). Both phases display a range of $\delta^7\text{Li}$ values similar to those of the pyroxene rims (Table 2 and Fig. 7). $\delta^7\text{Li}$ values for maskelynites range between -1.5 and $+9.9$ ‰ whereas values for phosphates lie between -8.4 and $+6.5$ ‰. Even if there is an additional uncertainty of up to a few permil in the determination of the $\delta^7\text{Li}$ relative to pyroxenes of these two phases (see section 2), the $\delta^7\text{Li}$ values inferred for plagioclase and phosphates appear in agreement with their crystallization order during the differentiation (Barrat et al., 2002).

4. DISCUSSION

4. 1. Desert weathering of NWA 480

Hot desert weathering can significantly affect the trace element abundances of meteorites (Barrat et al., 1999, 2001, 2003; Stelzner et al., 1999; Crozaz and Wadhwa, 2001 and references therein). NWA 480 is no exception and a slight contamination by terrestrial light rare earth elements was previously detected in a few pyroxenes (Crozaz et al., 2001). Such effects should not be overemphasized, and it has been shown previously that NWA 480 is not severely weathered (Barrat et al., 2002). At the scale of a crystal, hot desert weathering introduces contaminants localized near fractures. The two profiles performed in a large pyroxene crystal, show neither anomalous Li concentration nor abnormal $\delta^7\text{Li}$ value near cracks or fractures (Fig. 5, Table 1). Furthermore, weathering processes are not expected to generate a regular $\delta^7\text{Li}$ core/rim zoning without disturbing Li abundances in a roughly correlated way. We conclude that the Li abundances and isotopic ratios in NWA 480 mineral phases are pre-terrestrial, and thus reflect magmatic or post-magmatic processes.

4. 2. Li behavior during closed system fractional crystallization

Two lines of argument indicate that the Li systematics observed in NWA 480 pyroxenes cannot be the result of closed system fractional crystallization. First, the near constancy of Li concentrations in pyroxene is contrary to that predicted for an incompatible element. The experimental Li partition coefficients obtained for ferromagnesian silicates and plagioclase indicate that Li is incompatible during the crystallization of dry basaltic systems (Brenan et al., 1998a; Herd et al., 2002). Assuming crystallization in a closed-system, an increase of concentrations from core to the rim of the pyroxene and a correlation with

Fe/(Fe+Mg) are expected for incompatible elements. Such a behavior is observed for example for Ti in NWA 480 pyroxenes (Barrat et al., 2002) but not for Li (Fig. 5 and 6)

Second, the range of $\delta^7\text{Li}$ values displayed by the NWA 480 pyroxenes, about 25 ‰, is huge, astonishing within a single crystal, and not compatible with what is known for crystal/melt Li isotopic fractionations in terrestrial rocks. In fact, an equilibrium Li isotopic fractionation of at maximum 2 ‰ can be anticipated between crystal and melt in fluid-poor basaltic systems, as indicated by samples from the Kilauea Iki lava lake in Hawaii (Tomascak et al., 1999). In addition, compared to terrestrial mantle lavas, the range observed in NWA 480 is about 6 times larger than the variations displayed by Mid Ocean Ridge Basalts (MORBs) and about 1.5 times larger than those of Oceanic Island Basalts (OIBs) (Chan et al., 1992; Chan and Frey, 2003; Decitre and Deloule, 2003).

4. 3. Interaction with magma and/or fluids in the Martian crust ?

The large range of $\delta^7\text{Li}$ values imply that the differentiation of NWA 480 parental melts occurred in an open system. Mixing of two magmas with different $^7\text{Li}/^6\text{Li}$ ratios or assimilation of a component by the magma (e.g. Assimilation-Fractional Crystallization (A.F.C.), DePaolo, 1981) are a priori both able to generate a wide range of Li isotopic compositions. In the present case, these processes seem unlikely. Nothing in the behavior of major, minor (Cr, Al, Ti, Na) or trace elements (Zr, Y, REEs) in the pyroxenes (Fig. 6) suggests the involvement of mixing and/or contamination processes (Crozas et al., 2001; Barrat et al., 2002). Furthermore, such processes would fail to explain (i) the decoupling observed between Li abundances and $\delta^7\text{Li}$ values and (ii) that most of the $\delta^7\text{Li}$ -range is observed in a rather homogenous part of the Mg-rich core of the pyroxene. In addition, the lack of knowledge of Li isotopic variations in the Martian crust hampers any detailed modeling of the contamination of the NWA 480 parental melt. Finally, it is important to stress

that mixing of fluid-poor basaltic melts, or A.F.C., would still result in an incompatible behavior of Li, which is clearly not what is observed in NWA 480 pyroxenes.

An alternative to A.F.C. could be the addition of an aqueous fluid to NWA 480 parental melt during its differentiation. In such a case, Li would preferentially partition into the fluid phase, which could buffer the magma lithium concentration in case of a closed system crystallization. In order to explain the enrichment in heavy Li isotope seen from pyroxene core to rim in NWA 480, this fluid should have a high $\delta^7\text{Li}$ to buffer the $\delta^7\text{Li}$ of the melt to a value of at least +10 ‰ (the $\delta^7\text{Li}$ value of the pyroxene rim). Such a process cannot be firmly excluded from the present data set but it faces major difficulties. Firstly, there is no observational or theoretical ground to call for high $\delta^7\text{Li}$ values for magmatic/hydrothermal fluids in the Martian crust. Furthermore, experimental phase relations on Shergotty at 56 MPa and 1120°C (Dann et al., 2001) suggest that this shergottite crystallized in rather hydrous conditions but with a small amount of water (H₂O concentration of the melt ~1.8 wt%) in order to reproduce the observed co-crystallization of pigeonite and augite. Thus the crystallization of NWA 480 under fluid saturated conditions, if it may explain the observed Li isotopic variations in case of a ⁷Li-rich fluid, is not consistent with the petrology of this rock.

4. 4. Diffusion-induced kinetic fractionation

Experimental work has shown that lithium is one of the fastest diffusing elements in silicate melt (Mungall, 2000) and the large mass difference between the two isotopes (~17 %) implies a large difference in diffusion speed between ⁷Li and ⁶Li. Therefore, reequilibration of a Li gradient can produce a strong isotopic fractionation. However, for such a mechanism to be efficient and preserved in a 200 μm wide pyroxene, an incredibly fast cooling rate of the crystal is needed, less than a few minutes (using $D_{\text{Li}} = 6 \cdot 10^{-6} \text{ cm}^2/\text{s}$, value for a tholeiitic melt; Lundstrom, 2003). This is obviously not consistent with the 0.5°C/h estimated cooling rate

from pyroxene major element zoning (Barrat et al., 2002). Finally, if a diffusion induced kinetic isotopic fractionation was responsible of the observed $\delta^7\text{Li}$ variations in NWA 480 pyroxene it is necessary for a residual Li abundance gradient to be preserved from core to rim. This is not observed in the Li concentration profile (Fig. 5) so that diffusion-induced isotopic fractionation seems not responsible for the Li isotopic variability observed in NWA 480 pyroxenes.

4. 5. Degassing of NWA 480 parental melt

When fluid phases exsolve from magma, they react with it, and can mobilize soluble trace element species. Because Li has a strong affinity with aqueous fluids (e.g. Brenan et al., 1998b), the effects of water degassing have to be considered. For Zagami and Shergotty, Lentz et al. (2001) suggested that Li was mobilized by fluids and lost from the magma during crystallization: this resulted in a decrease of Li contents from core to rim. Such a distribution of Li in pyroxene was proposed as a criterion for water degassing. Because of the large scatter in the Shergotty and Zagami data it is possible to interpret Li variations either as reflecting two distinct stages (high Li /low Li) or a progressive decrease in Li concentrations. Therefore, it is not possible to make a distinction between instantaneous and progressive degassing.

In the case of NWA 480, Li concentrations are constant from pyroxene core to rim. A combination of a progressive degassing and crystal fractionation can result in more or less constant Li concentrations in the melt so that the traces of degassing could be partly obscured. However, a more robust criterion for degassing might be the Li isotopic composition since a significant isotopic fractionation can be anticipated for Li between the fluid and the melt, with a ^7Li -enrichment in the residual melt during degassing. In this hypothesis the pristine $\delta^7\text{Li}$ value of the magma may correspond to that of the pyroxene cores ($\delta^7\text{Li} = -17 \text{ ‰}$). Note that

this value is much lower than for bulk chondrites (McDonough et al., 2003) or the terrestrial mantle (Tomascack et al., 1999).

In the following, a degassing process is tentatively quantified from two different constraints: (i) from the constancy of Li contents and (ii) from the range of Li isotopic variations.

In order to estimate the behavior of Li in a dry shergottitic melt, it is necessary to find an element having the same incompatibility behavior as Li but which is insoluble in aqueous fluid. Although being an alkali element like Li, Na may be compatible in plagioclase contrary to Li so that its concentration variation in the melt may not mimic that of Li. Titanium seems a better choice since experimental studies have shown that the partition coefficients of Ti and Li are quite similar for augite and pigeonite ($D_{Li} \approx D_{Ti} \approx 0.20$, Brenan et al., 1998a; McCoy and Lofgren, 1999; Herd et al., 2002). Assuming that the system is closed, we can infer that the zoning of Li and Ti abundances recorded by the growing pyroxene crystals may be parallel.

Therefore, the Ti abundances in pyroxenes can be used to estimate the amount of Li lost during the differentiation. During the crystallization of the pyroxene core, from $fe\# = 21$ to 30, TiO_2 abundances increase from about 0.05 to 0.15-0.20 wt%. The Li abundances should then increase from 3.2 $\mu g/g$ in the core to approximately 10-13 $\mu g/g$ at $fe\# = 30$. These results contrast with the 3.5 $\mu g/g$ of Li observed for $fe\# = 30$ and suggest that approximately 65-75 % of the Li has been lost by the system.

Assuming that a degassing process is responsible for the Li isotopic variations recorded by the pyroxene cores, a first order estimate of the amount of Li lost by the magma can be made using a simple Rayleigh distillation law:

$$(\delta^7Li)_{\text{magma}} = [(\delta^7Li)_0 + 1000] F^{\alpha-1} - 1000 \quad (1)$$

where $(\delta^7\text{Li})_{\text{magma}}$ and $(\delta^7\text{Li})_0$ are the $\delta^7\text{Li}$ -values of the degassed magma and of the initial magma respectively, α the isotopic fractionation factor between vapor and melt, and F the fraction of Li remaining in the magma. Unfortunately, the values of α and the Li speciation in magmas and fluids, have not yet been determined experimentally. Thus, α -values can only be guessed on theoretical grounds. It can be anticipated that they will differ if Li is carried away in the gas from the magma as elemental (Li), oxide (Li_2O), chloride (LiCl) or sulfide (Li_2S) gas species. While the equilibrium fractionation factor between vapor and melt is not known but is probably rather low, the kinetic isotopic fractionation can be estimated for different species in the melt as the square root ratio of the masses of fractionating species (Davis et al., 1990). For the sake of exercise, the values of α can be approximated for Li_2O and Li_2S by 0.966 and 0.978, respectively. Calculations indicate that the system should have lost about 51-66 % of its initial Li in order to reproduce the increase of $\delta^7\text{Li}$ values (from -17 to $+7$ ‰) recorded by the pyroxene crystals between $fe\# = 21$ to 30. This amount of Li is in good agreement with that calculated above to reproduce the constancy of Li concentrations in pyroxene. Therefore it can be concluded that, at least at first order, coupled degassing-fractionation of NWA 480 parental melts can explain the Li systematics observed in Fe-poor pyroxenes.

For $fe\# > 30$, the behavior of Li is not clear. Pyroxene rims co-crystallized with plagioclase and phosphates. Li is still incompatible during the crystallization of these phases (Herd et al., 2003). The few Li abundances that were determined do not indicate a change in the Li behavior but the $\delta^7\text{Li}$ values seem to reach a maximum value near $+7$ ‰, and present a quite large scatter (± 4 ‰). This large scattering is also observed for plagioclase and phosphates (Fig. 7). The simple degassing model fails to explain these observations and a secondary mechanism has to be considered. Two distinct hypothesis can be proposed (i) periodic additions of fluid with various $\delta^7\text{Li}$ (ii) partial resetting of $\delta^7\text{Li}$ compositions

occurred during shock event inducing partial Li isotopic reequilibration of plagioclase and phosphate with pyroxene rims, erasing the degassing signature. The lack of experimental data prevents any quantitative assessment of such processes.

5. CONCLUSIONS

The present ion microprobe study revealed the presence of a large Li isotopic zoning (of about 25‰) in pyroxenes from the shergottite NWA 480. Contrary to Shergotty and Zagami, the Li concentrations are rather constant from core to rim in NWA 480 pyroxenes, which indicates that Li was not fractionated in a dry closed system. Neither terrestrial weathering processes, nor fractional crystallization (or assimilation-fractional crystallization) can account for these observations. On the contrary degassing of the magma can reasonably induce mass-fractionation between the two Li isotopes, leading to an increase of $\delta^7\text{Li}$ in the remaining magma and maintaining its Li content rather constant during fractionation. A simple first order modeling of these processes show that the constancy of Li contents and the range of Li isotopic compositions can be obtained for a Li loss from the magma of approximately 50-70 %.

Evidence for degassing was previously discussed using B and Li abundances in pyroxenes in Shergotty and Zagami (Lentz et al., 2001). The present work shows that degassing may also have acted in a shergottite petrologically distinct from them. Further work must be performed on well-constrained terrestrial systems, in order to fulfill the lack of data on Li isotopic fractionation during degassing. Li isotopes seem to be a powerful recorder of the degassing of magmas.

Acknowledgments- The technical help of D. Mangin, M. Champenois and C. Rollion-Bard during the SIMS sessions has been appreciated. We thank David Mittlefehldt for the editorial handling, Allan Treiman, and the two anonymous reviewers for constructive comments. We

thank Martin Palmer for a review of a draft of this paper. We gratefully acknowledge the Programme National de Planétologie (CNRS-INSU) for financial support. This research has made use of NASA's Astrophysics Data System Abstract Service.

References

- Barrat J. A., Gillet Ph., Lesourd M., Blichert-Toft J., and Poupeau G. R. (1999) The Tatahouine diogenite: Mineralogical and chemical effects of sixty-three years of terrestrial residence. *Meteoritics Planet. Sci.* **34**, 91-97.
- Barrat J. A., Blichert-Toft J., Nesbitt R. W. and Keller F. (2001) Bulk chemistry of saharan shergottite Dar al Gani 476. *Meteoritics Planet. Science* **36**, 23-29.
- Barrat J. A., Gillet Ph., Sautter V., Jambon A., Javoy M., Göpel C., Lesourd M., and Petit E. (2002) Petrology and geochemistry of the basaltic shergottite NWA 480. *Meteoritics Planet. Sci.* **37**, 487-499.
- Barrat J. A., Jambon A., Bohn M., Blichert-Toft J., Sautter V., Göpel C., Gillet Ph., Boudouma O., and Keller F. (2003) Petrology and geochemistry of the unbrecciated achondrite Northwest Africa 1240 (NWA 1240): an HED parent body impact melt. *Geochim. Cosmochim. Acta* **67**, 3959-3970.
- Borg L. E., Nyquist L. E., Wiesmann H. And Reese Y. (2002) Constraints on the petrogenesis of Martian meteorites from the Rb-Sr and Sm-Nd isotopic systematics of the lherzolithic shergottites ALH77005 and LEW88516. *Geochim. Cosmochim. Acta.* **66**, 2037-2053.
- Brenan J. M., Neroda E., Lundstrom C. C., Shaw H. F., Ryerson F. J. and Phinney D. L. (1998a) Behaviour of boron, beryllium, and lithium during melting and crystallization: constraints from mineral melt partitioning experiments. *Geochim. Cosmochim. Acta* **62**, 2129-2141.
- Brenan J. M., Ryerson F. J. And Shaw H. F. (1998b) The role of aqueous fluids in the slab-to-mantle transfer of boron, beryllium and lithium during subduction: experiments and models. *Geochim. Cosmochim. Acta* **62**, 3337-3347.
- Chan L. H., and Frey F. A. (2003) Lithium isotope geochemistry of the Hawaiian plume: results from the Hawaii Scientific Drilling Project and Koolau Volcano. *Geochem. Geophys. Geosyst.* **4**, 10.1029/2002GC000365
- Chan L. H., Edmond J. M., Thompson G. and Gillis K. (1992) Lithium isotopic composition of submarine basalts – Implications for the lithium cycle in the oceans. *Earth Planet. Sci. Lett.* **108**, 151-160.
- Chaussidon M. and Robert F. (1998) $^7\text{Li}/^6\text{Li}$ and $^{11}\text{B}/^{10}\text{B}$ variations in chondrules from the Semarkona unequilibrated chondrite. *Earth Planet. Sci. Lett.* **164**, 577-589.

- Chaussidon M., Robert F., Mangin D., Hanon P. and Rose E. F. (1997) Analytical procedures for the measurement of boron isotope compositions by ion microprobe in meteorites and mantle rocks. *Geostandards Newsletter* **21**, 7-17.
- Crozaz G., and Wadhwa M. (2001) The terrestrial alteration of Saharan shergottites Dar al Gani 476 and 489: a case study of weathering in a hot desert environment. *Geochim. Cosmochim. Acta* **65**, 971-978.
- Crozaz G., Wadhwa M., and Barrat J. A. (2001) Trace elements in NWA 480: still more diversity in the basaltic shergottite group. *Meteoritics Planet. Sci.* **36**, A45.
- Dann J. C., Holzheid A.H., Grove T. L. and McSween H. Y. Jr. (2001) Phase equilibria of the shergotty meteorite: Constraints on pre-eruptive water contents of martian magmas and fractional crystallization under hydrous conditions. *Meteoritics Planet. Sci.* **36**, 793-806.
- Davis A. M., Hashimoto A., Clayton R. N. and Mayeda K. (1990) Isotope mass-fractionation during evaporation of Mg₂SiO₄. *Nature* **347**, 655-658.
- Decitre S. and Deloule E. (2003) Li isotopic compositions of oceanic basaltic glasses: implications for the Li isotope compositions of the mantle. *Earth Planet. Sci. Lett.* In press.
- Decitre S., Deloule E., Reisberg L., James R., Agrinier P. and Mevel C. (2002) Behaviour of Li and its isotopes during serpentinization of oceanic peridotites. *Geochem. Geophys. Geosyst.* **3**, 10.1029/2001GC000178.
- DePaolo D. J. (1981) Trace-element and isotopic effects of combined wallrock assimilation and fractional crystallisation. *Earth Planet. Sci. Lett.* **53**, 189-202.
- Flesh G. D., Anderson A. R. and Svec H.J. (1973) A secondary isotopic standard for ⁷Li/⁶Li determination. *Int. J. Mass Spectro. Ion Phys.* **12**, 265-272
- Herd C. D. K., Treiman A. H., McKay G. A. and Shearer C. K. (2002) Implications of experimental lithium and boron partition coefficients for the petrogenesis of Martian basalts. *Meteoritics Planet. Sci.* **37**, A62.
- Herd C. D. K., Treiman A. H., McKay G. A. and Shearer C. K. (2003) Light lithophile elements in natural and experimental phases in martian basalts: implications for the degassing of water from martian magmas. *Lunar Planet. Sci.* **34**, #1635.
- Hinton R. W. (1990) Ion microprobe trace-element analysis of silicates. Measurements of multi-element glasses. *Chem. Geology.* **83**, 11-25.
- Lentz R. C. F., McSween H. Y. Jr, Ryan J. and Riciputi L. R. (2001) Water in Martian magmas: clues from light lithophile elements in shergottite and nakhlite pyroxenes. *Geochim. Cosmochim. Acta* **65**, 4551-4565.

- Lundstrom C. C., (2003) Further investigation of the diffusive infiltration of alkalis into partially molten peridotite: implications for upper mantle melting and anomalous Cl rich melt inclusions in MORB. *Geochem. Geophys. Geosyst.* **4**, 10.1029/2001GC000224.
- McCoy T. J. and Lofgren G. E. (1999) Crystallization of the Zagami shergottite: an experimental study. *Earth Planet. Sci. Lett.* **173**, 397-411.
- McDonough W. F., Teng F. Z., Tomascak P. B., Ash R. D., Grossman J. N., Rudnick R. L. (2003) Lithium isotopic composition of chondritic meteorites. *Lunar Planet. Sci.* **34**, #1931.
- McSween H. Y. Jr (2002) The rocks of Mars, from far and near. *Meteoritics Planet. Sci.* **37**, 7-25.
- McSween H. Y. Jr, Grove T. L., Lentz R. C. F., Jesse C., Dann C., Holzheid A. H., Riciputi L. R. and Ryans J. G. (2001) Geochemical evidence for magmatic water within Mars from pyroxenes in the Shergotty meteorite. *Nature* **409**, 487-490.
- Mungall J. E. (2002) Empirical models relating viscosity and tracer diffusion in magmatic silicate melts. *Geochim. Cosmochim. Acta* **66**, 125-143.
- Stelzner T., Heide K., Bischoff A., Weber D., Scherer P., Schultz L., Happel M., Schrön W., Neupert U., Michel R., Clayton R. N., Mayeda T. K., Bonani G., Haidas I., Ivy-Ochs S., and Suter M. (1999) An interdisciplinary study of weathering effects in ordinary chondrites from the Acfer region, Algeria. *Meteoritics Planet. Sci.* **34**, 787-794.
- Tomascak P. B., Tera F., Heltz R. T. And Walker R. J. (1999) The absence of lithium isotope fractionation during basalt differentiation: New measurement by multicollector sector ICP-MS. *Geochim. Cosmochim. Acta* **63**, 907-910.
- Treiman A. H., Gleason J. D., and Bogard D. D. (2000) The SNC meteorites are from Mars. *Planet. Space Sci.* **48**, 1213-1320.
- Wadhwa M. (2001) Redox state of Mars upper mantle and crust from Eu anomalies in shergottite pyroxenes. *Science* **291**, 1527-1530.
- Wadhwa M., McSween H. Y. Jr, and Crozaz G. (1994) Petrogenesis of shergottite meteorites inferred from minor and trace element microdistributions. *Geochim. Cosmochim. Acta* **58**, 4213-4229.
- Wadhwa M., Lentz R. C. F., McSween H. Y. Jr., and Crozaz G. (2001) A Petrologic and trace element study of Dar al Gani 476 and Dar al Gani 489: twin meteorites with affinities to basaltic and lherzolitic shergottites. *Meteoritics Planet. Sci.* **36**, 195-208.

#	En	Wo	Fs	$\frac{100 \text{ Fe}}{\text{Fe+Mg}}$	TiO ₂ (wt %)	Al ₂ O ₃ (wt %)	Li ($\mu\text{g/g}$)	$\delta^7\text{Li} (\pm 1 \sigma)$ (‰)
Pyroxene 1, profile A-B								
2	57.1	11.4	31.5	35.53	0.13	0.56	3.5	+2.3 ± 1.6
3	47.3	17.2	35.5	42.88	0.39	1.02	3.2	-3.9 ± 1.5
4	57.1	9.1	33.8	37.18	0.27	0.67	3.0	+0.4 ± 1.4
5	64.3	7.6	28.2	30.48	0.15	0.62	3.4	+8.5 ± 1.3
6	57.7	7.4	34.9	37.70	0.19	0.63	4.0	+1.5 ± 1.7
7	70.8	4.8	24.4	25.63	0.10	0.43	3.5	-4.8 ± 1.3
8	73.0	3.6	23.4	24.27	0.13	0.40	3.2	+2.1 ± 1.4
9	73.3	3.6	23.1	23.96	0.10	0.39	3.4	-1.6 ± 1.4
10	73.2	3.5	23.3	24.15	0.09	0.41	3.2	-11.2 ± 1.2
11	73.9	3.4	22.8	23.57	0.07	0.35	3.4	-16.6 ± 1.4
12	73.9	3.4	22.7	23.48	0.05	0.34	5.5	-17.3 ± 1.4
13	74.0	3.4	22.6	23.41	0.05	0.35	3.9	-15.1 ± 1.6
14	73.8	3.4	22.9	23.67	0.10	0.32	3.7	-14.6 ± 1.2
15	73.3	3.4	23.3	24.13	0.08	0.35	3.5	-12.9 ± 1.3
16	72.7	3.8	23.5	24.39	0.05	0.39	3.6	-8.0 ± 1.5
17	71.0	4.3	24.7	25.82	0.12	0.44	3.3	-6.7 ± 1.2
18	70.5	4.2	25.3	26.44	0.12	0.37	3.8	-0.8 ± 1.2
19	66.1	6.1	27.8	29.62	0.10	0.43	3.8	+4.1 ± 1.2
20	62.9	8.6	28.5	31.20	0.16	0.51	2.7	+4.6 ± 1.2
Pyroxene 1, profile C-D								
22	19.2	18.4	62.4	76.45	0.60	0.55	3.9	+9.8 ± 1.9
23	30.9	28.9	40.2	56.51	0.71	1.19		+1.5 ± 1.8
24	44.5	30.2	25.3	36.21	0.28	1.03	3.2	+6.3 ± 1.5
25	49.5	24.9	25.6	34.09	0.24	0.76	3.6	+1.9 ± 1.9
26	63.1	7.8	29.1	31.54	0.19	0.53	3.3	-4.6 ± 1.6
27	73.6	3.4	23.0	23.82	0.08	0.38	3.5	-6.2 ± 1.2
28	74.3	3.4	22.3	23.10	0.05	0.34	3.8	-16.5 ± 1.5
29	72.4	3.8	23.8	24.73	0.07	0.36		-8.1 ± 1.5
30	60.3	7.8	31.9	34.63	0.35	0.76		+1.7 ± 1.4
31	50.8	24.3	24.9	32.93	0.24	0.75	3.5	-0.5 ± 1.8
Pyroxene 2								
1 (core)	76.7	2.9	20.4	21.00	0.05	0.32		-17.7 ± 1.5
77 (rim)	11.1	15.6	73.2	86.79	0.55	0.39		+4.4 ± 1.9
Pyroxene 3								
55 (core)								-17.4 ± 2.1
56 (rim)	44.9	30.3	24.8	35.59	0.30	0.96		+2.3 ± 1.9
Pyroxene 4								
78	22.7	15.4	61.9	73.15	0.54	0.49	2.4	
79	25.3	17.8	56.9	69.24	0.51	0.63	2.7	
81	39.2	29.7	31.0	44.18	0.45	1.34	3.7	

Table 1. Representative chemical analyses and Li isotopic compositions of pyroxenes in NWA 480. The 1 σ error corresponds to the counting statistics.

#	$\delta^7\text{Li}$ (‰) ($\pm 1 \sigma$)
Maskelynite	
57	-1.5 ± 1.6
58	$+1.5 \pm 1.7$
32	$+0.5 \pm 1.8$
33	$+9.9 \pm 1.5$
34	$+8.6 \pm 1.3$
Phosphates	
74	-8.4 ± 1.7
75	$+1.2 \pm 2.4$
76	$+6.5 \pm 3.9$
59	-1.5 ± 1.8
60	-1.9 ± 1.7
61	-2.2 ± 1.6
62	$+1.9 \pm 1.7$

Table 2. Li isotopic compositions of maskelynite and phosphate grains in NWA 480. The 1σ error corresponds to the counting statistics.

Figure captions

1. Determination of instrumental mass fractionation of Li isotopes ($\alpha_{\text{inst}}^{\text{Li}}$) from the analysis of three pyroxene standards of different chemical and isotopic compositions (see text). Error bar corresponds to 2σ .
2. Back-Scattered-Electron image of a polished section of NWA 480. Large gray crystals are zoned pyroxene, and dark phase is maskelynite. Fe-Ti oxides, pyrrhotite, and chromite appear white. The two measurement profiles are indicated. The diameters of the symbols correspond approximately to the ion-probe spot size.
3. Quadrilateral pyroxene composition of NWA 480. Filled circles represent the available analyses (~800 points, Barrat et al., 2002 and this study). Open circles are the compositions of the points analyzed for Li and $^7\text{Li}/^6\text{Li}$.
4. Variation of Li concentration relative to TiO_2 , in pyroxene from NWA 480 (filled circle), Shergotty and Zagami (Lentz et al., 2001).
5. Ferrosilite (Fs), wollastonite (Wo), Li and $\delta^7\text{Li}$ variations along the two profiles performed on a large pyroxene crystal (see Fig. 2).
6. Variations of TiO_2 , Al_2O_3 , Li and $\delta^7\text{Li}$ in pyroxenes from NWA 480 relative to atomic $\text{Fe}/(\text{Fe}+\text{Mg})$. Error bar corresponds to 2σ .
7. Lithium isotopic composition of the mineral phases in NWA 480. Error bar corresponds to 2σ .

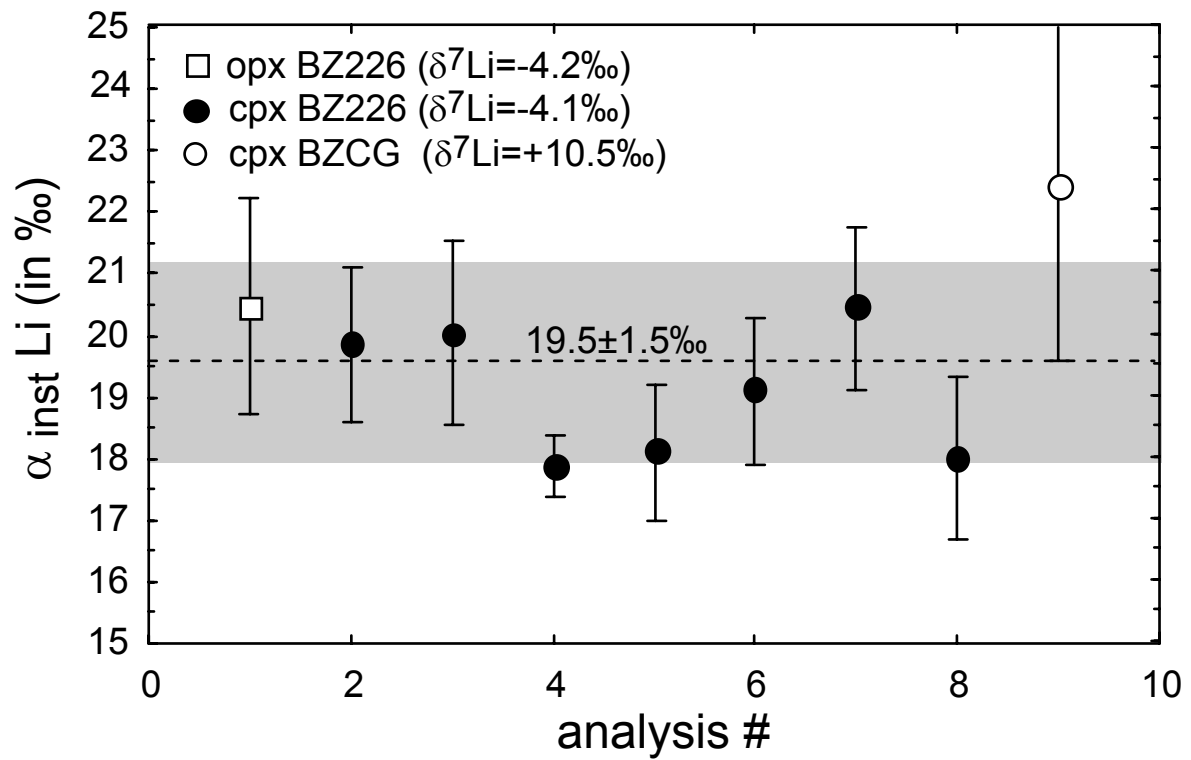


Fig 1. Determination of instrumental mass fractionation of Li isotopes ($\alpha_{\text{inst}}^{\text{Li}}$) from the analysis of three pyroxene standards of different chemical and isotopic compositions (see text). Error bar corresponds to 2σ .

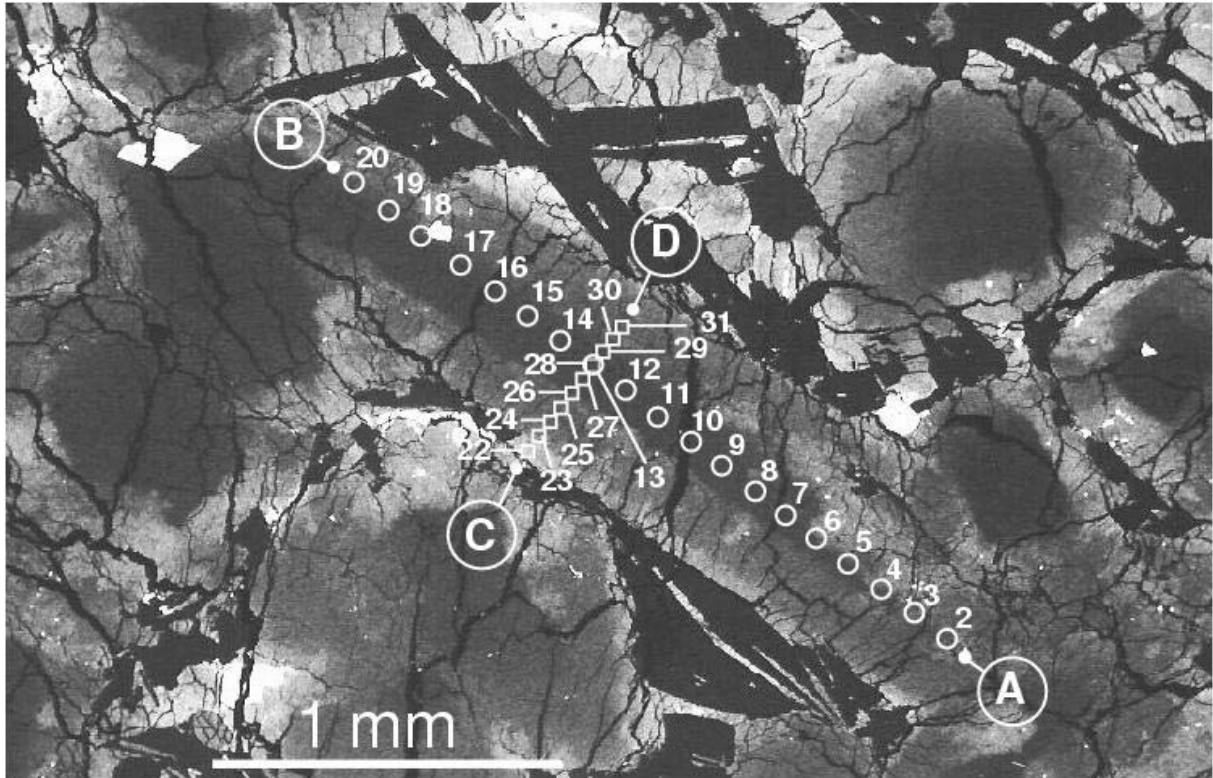


Fig 2. Back-Scattered-Electron image of a polished section of NWA 480. Large gray crystals are zoned pyroxene, and dark phase is maskelynite. Fe-Ti oxides, pyrrhotite, and chromite appear white. The two measurement profiles are indicated. The diameters of the symbols correspond approximately to the ion-probe spot size.

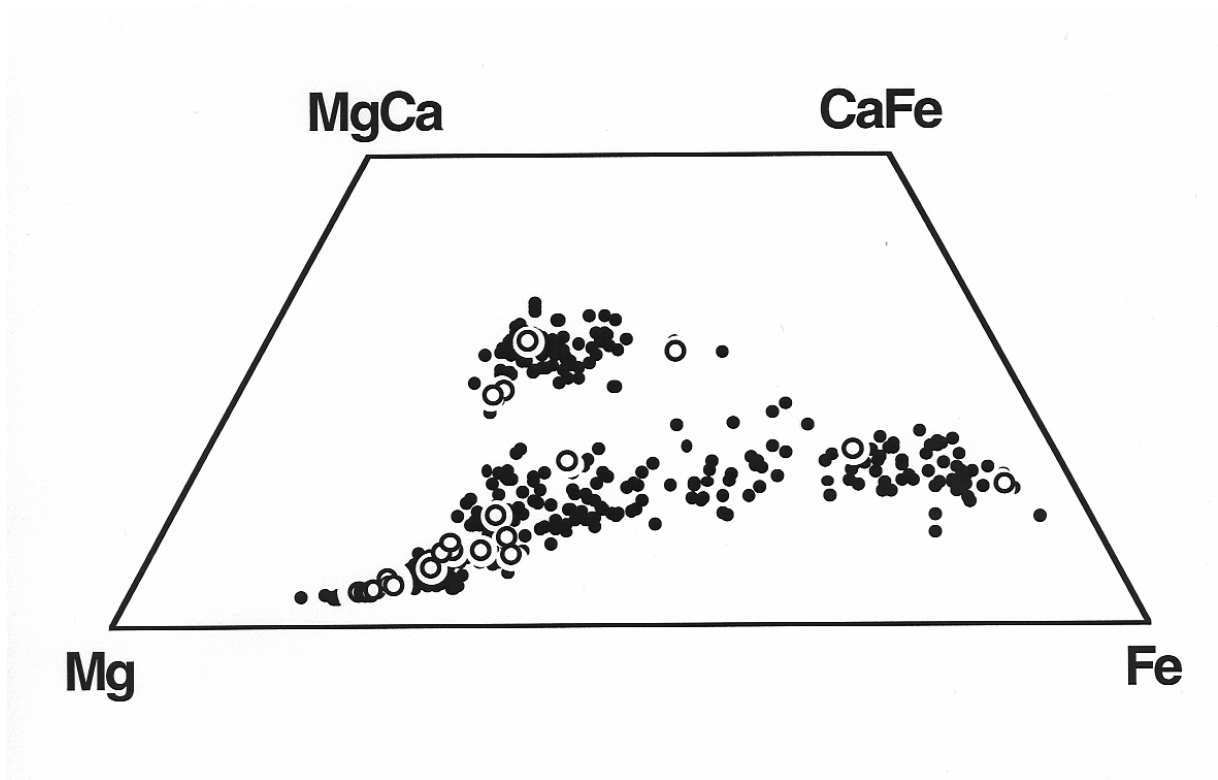


Fig 3. Quadrilateral pyroxene composition of NWA 480. Filled circles represent the available analyses (~800 points, Barrat et al., 2002 and this study). Open circles are the compositions of the points analyzed for Li and $^7\text{Li}/^6\text{Li}$.

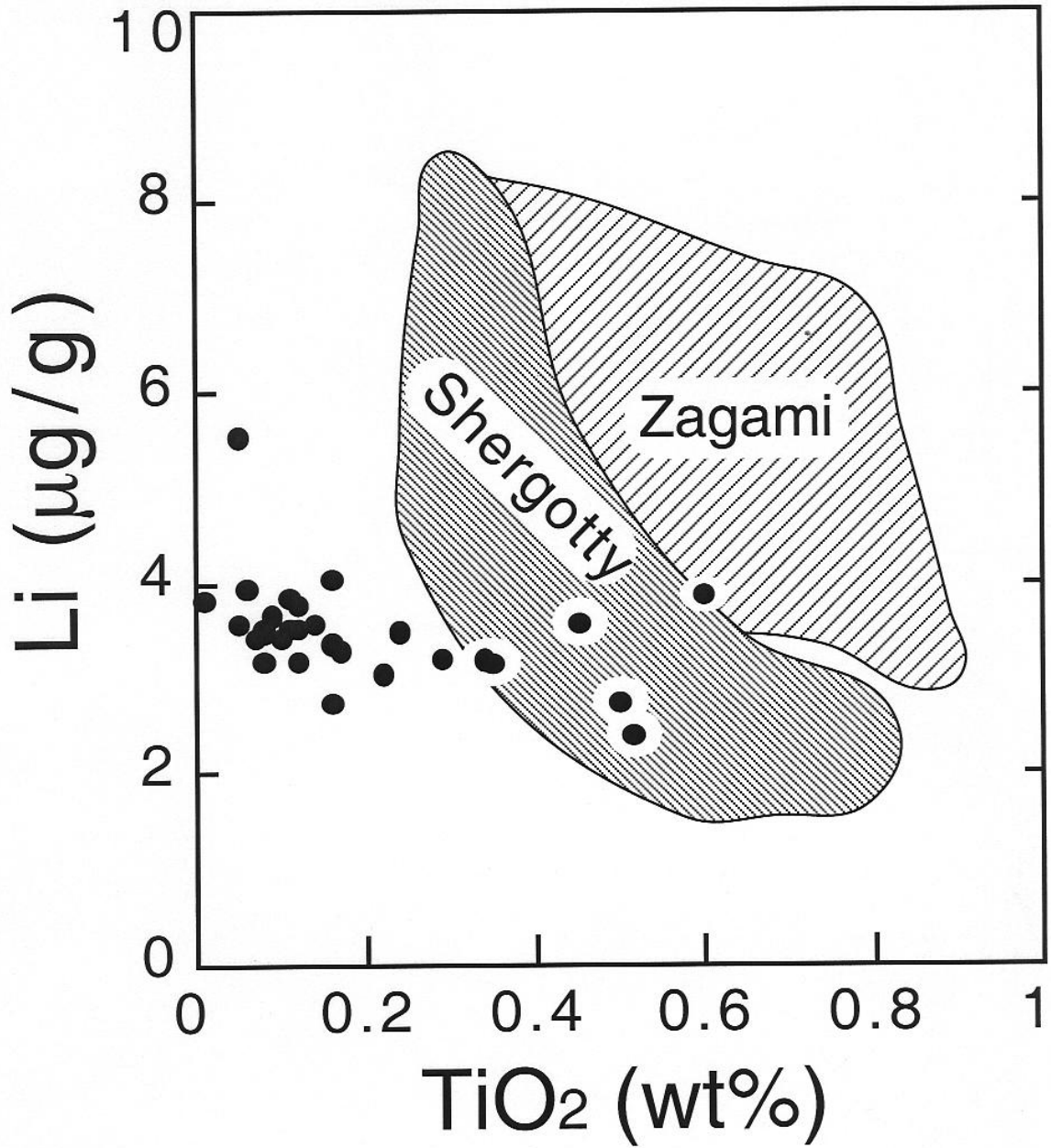


Fig 4. Variation of Li concentration relative to TiO_2 , in pyroxene from NWA 480 (filled circle), Shergotty and Zagami (Lentz et al., 2001).

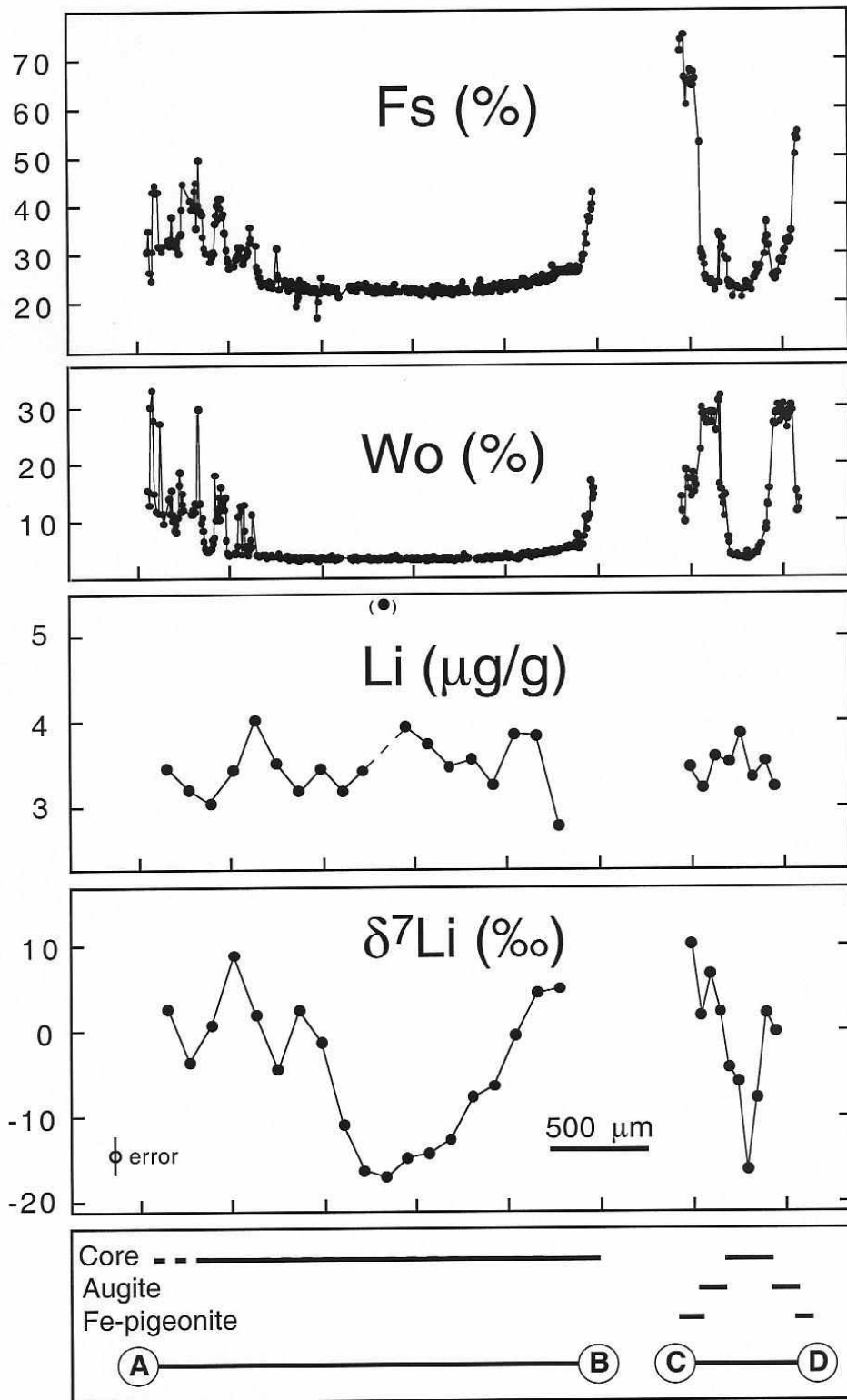


Fig 5. Ferrosilite (Fs), wollastonite (Wo), Li and $\delta^7\text{Li}$ variations along the two profiles performed on a large pyroxene crystal (see Fig. 2).

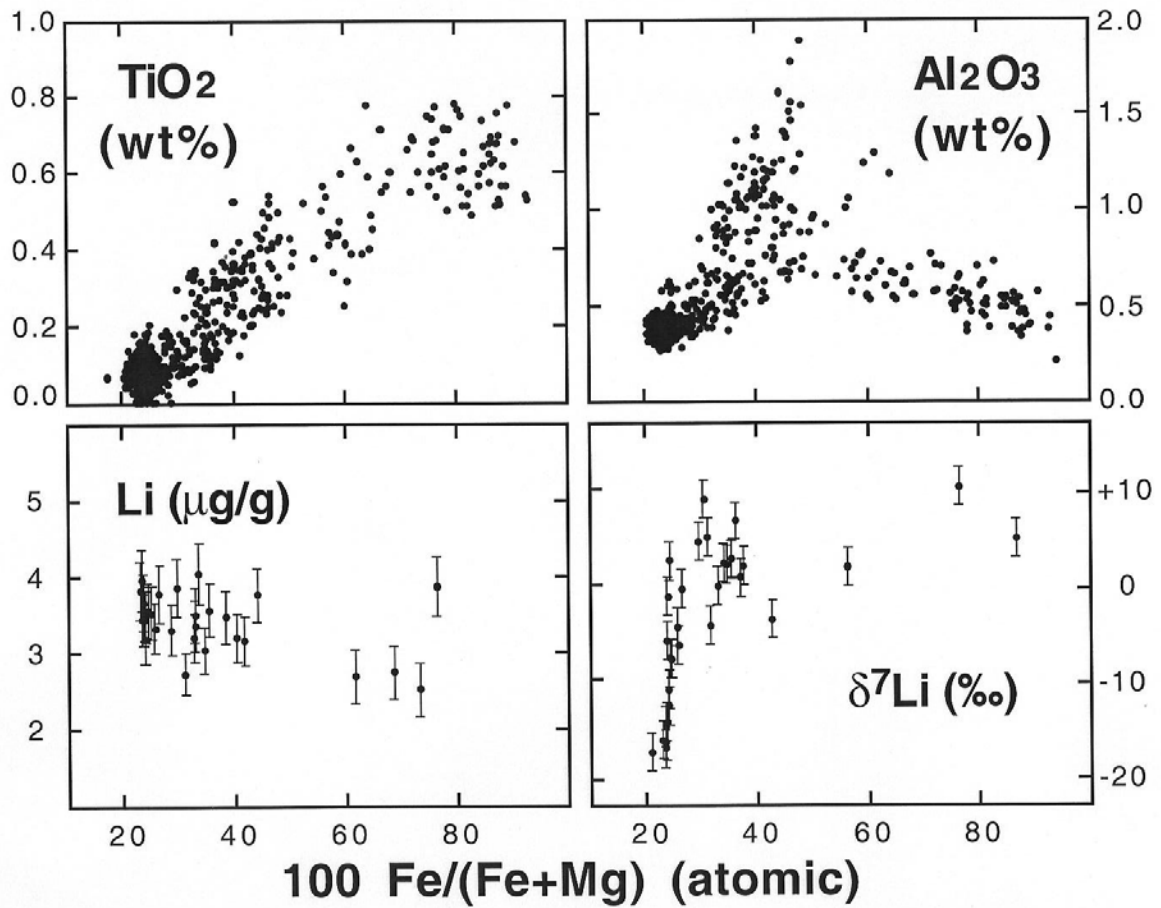


Fig 6. Variations of TiO₂, Al₂O₃, Li and δ⁷Li in pyroxenes from NWA 480 relative to atomic Fe/(Fe+Mg). Error bar corresponds to 2σ.

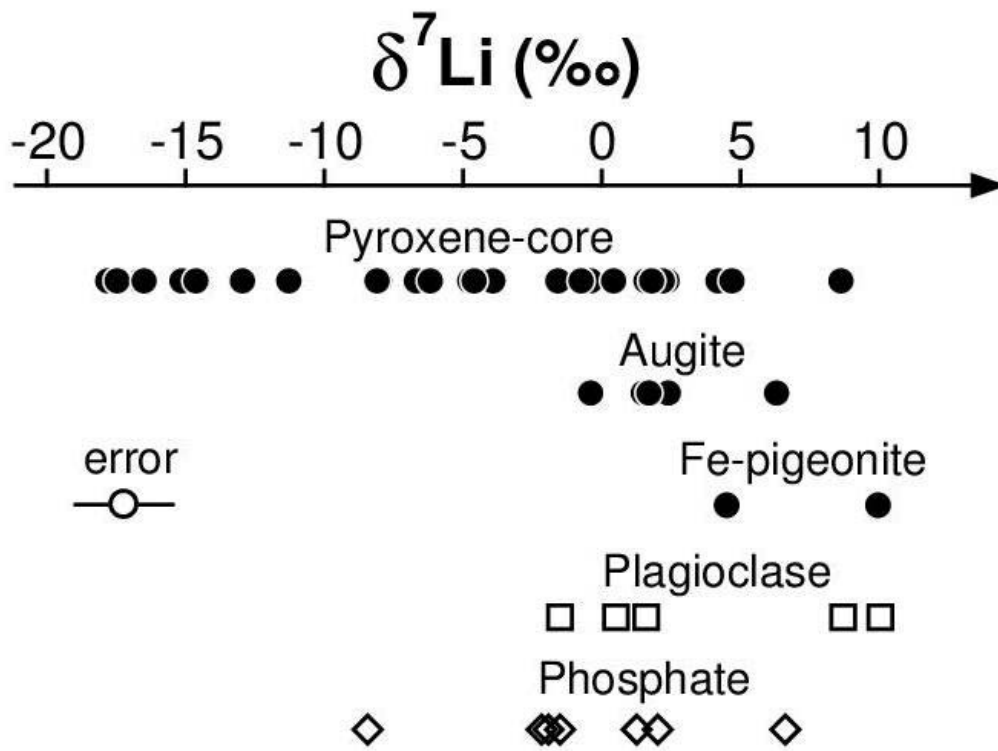


Fig 7. Lithium isotopic composition of the mineral phases in NWA 480. Error bar corresponds to 2σ .